Incorporation of Silica into Baroplastic Core-Shell Nanoparticles
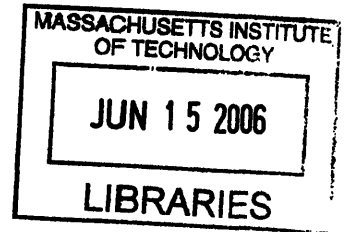
by

Sheldon A. Hewlett

Submitted to the Department of Materials Science and Engineering in Partial
Fulfillment of the Requirements for the Degree of

Bachelor of Science

At the
Massachusetts Institute of Technology

May 2006
[June 2006]

Signature of Author: _____
Department of Materials Science and Engineering
May 24th 2006

Certified by: _____
Anne M. Mayes
Toyota Professor of Materials Science and Engineering
Thesis Supervisor

Accepted by: _____
Caroline A. Ross
Professor of Materials Science and Engineering
Chair, Undergraduate Thesis Committee

Incorporation of Silica into Baroplastic Core-Shell Nanoparticles

by

Sheldon A. Hewlett

Submitted to the Department of Materials Science and Engineering
On May 24, 2005 in partial fulfillment of the requirements for the
Degree of Bachelor of Science

Abstract

Core-shell baroplastics are nanophase materials that exhibit pressure-induced flow at low temperatures and high pressures. Core-shell baroplastics used in this work are comprised of a low T_g poly(butyl acrylate) (PBA) core and a high T_g polystyrene (PS) shell. These novel polymer systems can be molded into fully formed, 3-D shapes with the application of high pressure at room temperature. While the mechanical properties are equivalent to or better than those of commercial thermoplastic elastomers, more can be done to improve upon individual aspects of the mechanical properties, such as elastic modulus.

This work looks at creating baroplastic nanocomposites with the goal of improving upon the mechanical properties. To accomplish this goal, two incorporation strategies for introducing silica nanoparticles were developed. The pre-emulsion strategy incorporated hydrophobized silica nanoparticles inside the core-shell nanoparticles to create core-shell-shell nanoparticles. The post-emulsion strategy incorporated charged silica nanoparticles after core-shell emulsion, with the intention of creating crystalline structures with silica and core-shell nanoparticles.

The pre-emulsion strategy resulted in a decrease in particle size for the core-shell-shell nanoparticles, as shown by dynamic light scattering. Excess silica in the emulsion resulted in phase separation and opaque, brittle samples. Samples made with this incorporation strategy showed poor mechanical properties. The post-emulsion strategy also resulted in poor processing. SAXS data show that there is no long range ordering with the SiO_2 and core-shell nanoparticles. However, SAXS did show the possibility of a nanopcomposite with short range ordering of silica and core-shell particles.

Thesis Supervisor: Anne M. Mayes
Title: Toyota Professor of Materials Science and Engineering

2

Index

List of Figures

List of Tables

Acknowledgements

I would like to thank Professor Anne Mayes for all of her teachings, guidance and patience with me, not only during this project, but in my time here at MIT. I will always appreciate the wealth of knowledge and advice she has given me in the three years I've been a part of Mayes Group.

None of this work would be possible without the amazing help from all of the Mayes Group members, past and present: Ayse Asatekin, Ozge Akbulut, William Kuhlman, Nathan Lovell, Solar Olugebefola, Elsa Olivetti, and Sang-Woog Ryu. I would especially like to thank Juan Gonzalez-Leon, for allowing me to be a part of this project, and for being a good mentor and even better friend.

Lastly, I would like to thank my parents for their never-ending support of me as I pursue my dreams. I continue to learn and grow so much from them, and will forever live by their unwavering example.

Chapter 1

BACKGROUND

1. 1 Baroplastics

Plastics recycling in the last twenty years has seen a number of improvements and changes, from an increased number of recycling plants in more communities to a more comprehensive sorting system for plastic waste. However, there are still downsides to the current recycling state. Plastic resins, when recycled, have a reduced number of uses as compared to their virgin products. Repeated heating of plastics causes thermooxidative break down of the polymer chains, and this reduces the structural integrity and usefulness of the recycled plastic.

To counteract this problem, novel polymer systems are currently being studied. One such system is the system of pressure miscible polymers which exhibit baroplastic behavior. Baroplastics are nanophase polymer systems which can under go low temperature processing at high applied pressure[1]. These systems are comprised of a low T_g component and a high T_g component. The harder, high T_g component provides the mechanical strength, and the softer, low T_g component offers the flexibility and formability at low temperatures. The advantages of baroplastics include low temperature processing with no degradation of the polymer chains, lower processing time with the removal of heating and cooling the mold apparatus, as well as reduced energy costs during processing.

1.1.1 Pressure induced miscibility in baroplastics

Pressure induced miscibility is a phenomenon in which phase separated polymer domains mix under the application of pressure[2-4]. In order to determine which polymer

components will mix, Ruzette and Mayes developed the compressible regular solution

model (CRS), which uses pure component properties to model the phase behavior of

binary polymers[5].

$$\Delta g_{mix} = kT\left[\frac{\phi_A \tilde{\rho}_A}{N_A v_A}\ln\phi_A + \frac{\phi_B \tilde{\rho}_B}{N_B v_B}\ln\phi_B\right] + \phi_A\phi_B\tilde{\rho}_A\tilde{\rho}_B\left(\delta_{A,0} - \delta_{B,0}\right)^2 + \phi_A\phi_B\left(\tilde{\rho}_A - \tilde{\rho}_B\right)\left(\delta_A^2 - \delta_B^2\right) \quad (1)$$

Where ϕ_i is the volume fraction of component i, $\tilde{\rho}_i$ is the reduced density (ratio of density

and hard core density), δ_i and $\delta_{i,0}$ are the solubility parameters of component i at T and

0K respectively, and N_i is the number of repeat units in the chain. While this model

predicts a phase diagram which is useful in determining phase separation behavior,

further use of the model was necessary in order to predict pressure induced miscibility.

This was done using the third term of the model, which arises from the differences of

thermal expansion of the polymers. This term was extrapolated to 0K to simulate the loss

of free volume, similar to the effect of compression upon pressure application. Systems

which exhibited a negative change in the third term value with respect to a drop in

temperature, such as poly(methylbutylene)/poly(ethylbutylene) (PMB/PEB) and

polystyrene/poly(butyl acrylate) (PBA), were expected to exhibit pressure induced

miscibility. On the other hand, systems that exhibited a positive change in third term

value, such as polystyrene/polyisoprene (PS/PI) and polystyrene/poly(lauryl

methacrylate) (PS/PLMA) were expected to exhibit pressure-induced demixing[6].

8
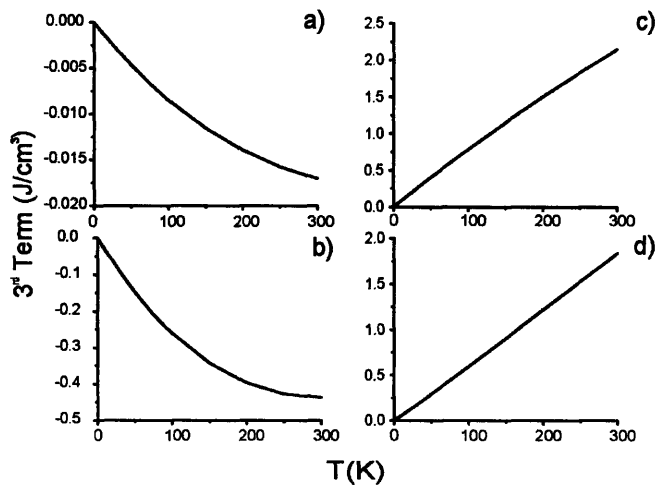
Figure 1-1. 3rd term values for pressure-miscible systems a) PMB/PEB b) PS/PBA and pressure demixing systems c) PS/PI and d) PS/PLMA[6]

Using the CRS model, it was determined that polystyrene (PS) combined with either

poly(butyl acrylate) (PBA) or poly(ethylhexyl acrylate) (PEHA) should theoretically

exhibit pressure-induced miscibility, as shown in Figure 1-1.

1.1.2 Processing of core-shell baroplastics

In work done by Gonzalez-Leon et al., core-shell nanoparticles, as well as block

copolymers, were found to be suitable morphologies in creating baroplastics. The low T_g

inner core, normally PBA or PEHA, of the nanoparticles is surrounded by a shell of the

high T_g polystyrene component. These phase separated systems have controlled domain

contact on the order of nanometers, which facilitates flow with the application of

pressure. Fully formed, three dimensional shapes were able to be processed at low

temperature, high pressure conditions, as shown in Figure 1-2.
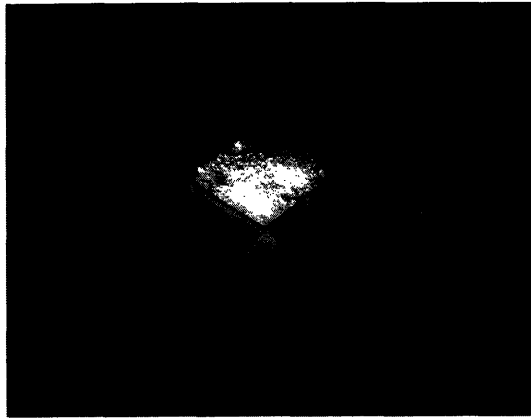
Figure 1-2. PS/PBA core-shell baroplastics processed at 25°C, 5000 psi, 1 min.[7]

Pressure-induced miscibility was seen to partially occur in these systems. Rather than completely mixing, the domains of high T_g and low T_g components were seen to partially mix at the interphase between two domains. This is evidenced in differential scanning calorimetry data where even after multiple processes, distinct domains are still present, as shown in Figure 1-3.
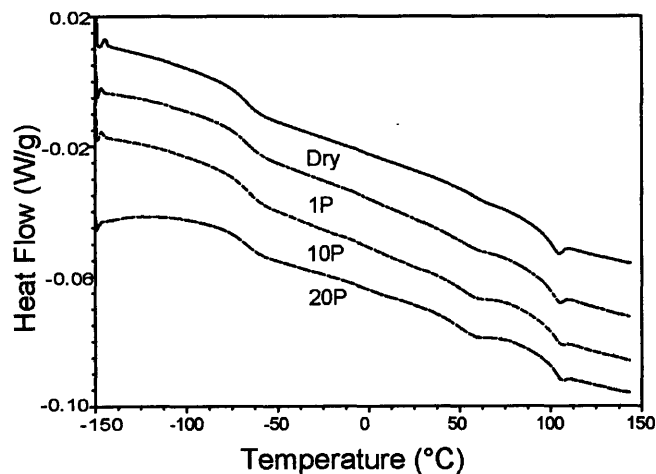
Figure 1-3. DSC data of PS/PEHA system as-dried and after processing 1, 2, 10, and 20 times. Two T_g values represent the unmixed high (~ 100°C) and low (~ -60°C) T_g components, while a middle T_g (~ 60°C) represents a mixed phase.[7]

10

1.1.3 Mechanical properties of baroplastic systems

The mechanical properties of baroplastics have been tested for a range of

compositions, processing times, and particle sizes. As seen in Figure 4, the mechanical

properties vary greatly with composition. Samples with high PS percentage but low PBA

percentage show a high elastic modulus, but a lower strain to break. In the reverse,

samples with a high PBA content, but a low PS content, showed strains that were outside

of the Instron range, yet very low modulus. This is consistent with what one would

expect to see, with the rubbery PBA content controlling the strain to break, and the

glassy PS percentage controlling the elastic modulus. All in all, the mechanical properties

of core-shell baroplastics are comparable with that of the block copolymer counterparts,

as is demonstrated in Figure 1-4. Table 1-1 provides elastic moduli of PS/PBA core shells

and thermoplastic elastomers styrene-isoprene-styrene (SIS) and styrene-butadiene (SB).
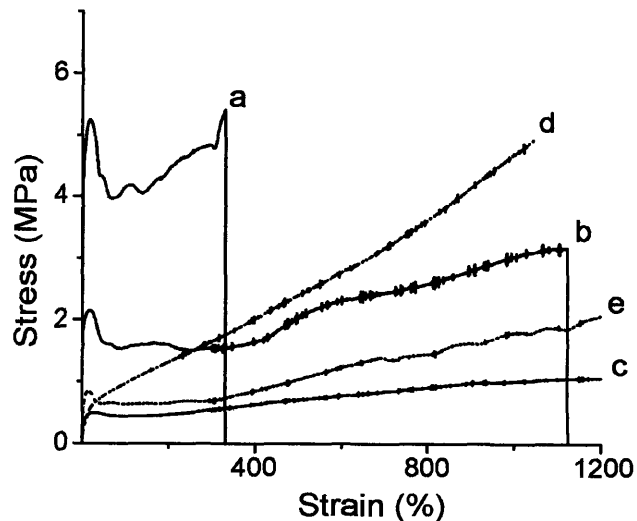
Figure 1-4. Stress vs strain curve for the core-shell baroplastics a) PBA_{42}/PS_{58}, b) PBA_{51}/PS_{49}, c) PBA_{59}/PS_{41} and commercial TPEs d) SIS and e) SB.[7]

Table 1-1. Elastic moduli for PS/PBA core shells and TPEs

Core/Shell or TPE	Elastic Modulus (MPa)
PBA_{59}/PS_{41}	13 ± 4
PBA_{51}/PS_{49}	96 ± 9
PBA_{42}/PS_{58}	215 ± 15
PS-b-PB	13 ± 3
PS-b-PI-b-PS	1 ± 0.4

While high T_g/ low T_g core-shell systems that don't exhibit pressure-induced miscibility can also be processed at low temperatures, they lack the interphase mixing that pressure miscible systems have. The mechanical properties of the pressure mixed systems as compared to the immiscible systems are superior, as shown in the tear strength tests in Figure 1-5. This is because the interphase between domains is reinforced through mixing.

Figure 1-5. a) Stress vs. strain and b) tear strength curves for PS/PBA (BS4) and non-pressure induced miscible PS/PLMA (LS1)[6]

1.2 Nanocomposites

Often when designing new materials, a good idea is to use combinations of inorganic (metals, ceramics) and organic (polymeric) materials to contribute different properties to the composite material. In nanocomposites, the combination of the inorganic and organic components is on the nanoscale, with resulting large interfacial area-to-volume ratios. The degree of dispersion and interfacial interaction of the inorganic material 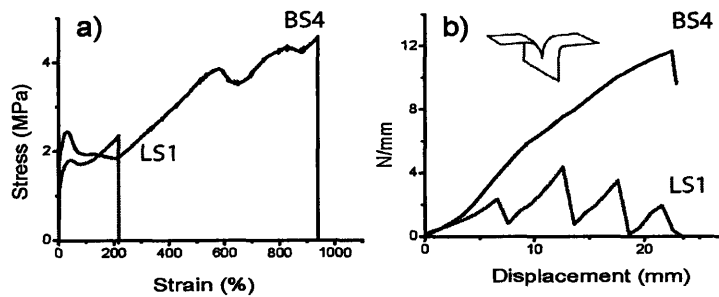in the polymeric material have a large effect on the bulk properties of nanocomposites. Through nanocomposites a wide variety of optical, electrical, magnetic, thermal, and mechanical properties associated with inorganic materials can be combined with the easy processability and flexibility of polymers[8].

1.2.1 Melt-mixed nanocomposites

Non-structured nanocomposites are those in which the inorganic nanoparticle component is incorporated by mixing methods, normally melt mixing into the polymer matrix. This method generally requires rather stringent mixing conditions, often with an extruder or other high energy mixing method. Dispersion of the inorganic material is often difficult, with aggregation and phase separation of the inorganic a likely outcome[9-10]. Surface modification of the inorganic phase is sometimes necessary in order to increase and promote homogeneous dispersion[9-10]. Some current work on nanocomposites includes melt mixing of SiO_2 nanoparticles into polymer matrices[9], or incorporation of $CaCO_3$ into Nylon to reduce thermal degradation[11].

1.2.2 Core-Shell nanocomposites

Especially useful in creating homogeneous nanocomposites are core-shell nanocomposites, where the inorganic nanoparticle is enclosed in a polymeric shell. The

encapsulation ensures that the inorganic component is well dispersed[8]. The polymer is

often synthesized using emulsion polymerization techniques. Surface modification of the

inorganic phase is often necessary in order to properly incorporate the nanoparticle into

the core of the polymer. In the research area of core shell nanocomposites, recent work

includes encapsulation of silica nanoparticles in poly(methyl methacrylate) (PMMA) or

polystyrene to create hollow spheres for antireflection coatings[12] (Fig.1-6), or

encapsulation of magnetic particles into polystyrene to obtain magnetized polymer

nanoparticles[13].
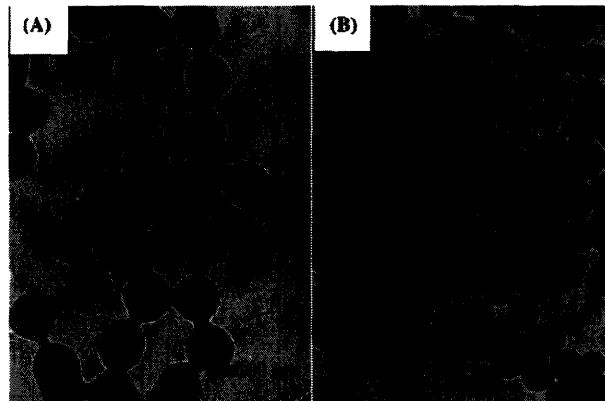
Figure 1-6. TEM images of SiO_2 encapsulated into a) PMMA and b) PS[12]

1.2.3 Baroplastic core-shells as potential nanocomposites

In continuing to improve upon baroplastics, the goal is to produce a plastic

that has the same mechanical and physical properties of more widely-used

thermoplastics, but with better recycling properties. As a result, several different avenues

to improve the mechanical properties of baroplastic core-shell particles have been

studied, including increased styrene composition, and processing at temperatures slightly

above room temperature[6]. Core-shell baroplastics make excellent precursors for

nanocomposites, since they already have the core-shell morphology, and the emulsion

14

polymerization allows for a relatively simple incorporation of other nanoparticles. Gonzalez-Leon has shown in his thesis work that incorporation of inorganic silica particles into the core-shell emulsion before precipitation produced a polymer that could still be processed at room temperature[6]. His findings show an increase in the Young's modulus of the incorporated silica baroplastic, indicating that inorganic materials could possibly be used to improve the mechanical properties of baroplastics. Including inorganic particles into the core-shell systems could also provide the baroplastics with added electrical, magnetic or optical properties. The focus of this thesis project is thus to further study the incorporation of inorganic materials, namely SiO_2, into core-shell baroplastics and the effect of the SiO_2 on the mechanical strength of the core-shell baroplastics.

Chapter 2 of this thesis will cover the synthesis, characterization, and processing methods utilized in this work. Hydrophobization, small angle x-ray scattering, and dynamic light scattering will all be discussed in this chapter. Chapters 3 and 4 will discuss the two incorporation points, pre-emulsion and post-emulsion respectively, with results of each incorporation scheme and subsequent processing results. Chapter 5 and 6 will discuss conclusions on this work and possible future work.

Chapter 2

Experimental Methods

2.1 Core-shell and core-shell-shell nanoparticle synthesis

Emulsion polymerization is one of a few different methods of creating spherical polymer particles. Emulsion polymerizations typically yield particles that are on the order of 100 to 500 nm, and involve a stabilizing surfactant, a monomer component and some dispersion media, usually water[14]. The exact nucleation method of the polymer particles is a topic that is still contested and undecided in the polymer research field. There are three widely accepted nucleation theories[14]. The micellar nucleation theory states that the polymer particles generally start from "swollen" surfactant micelles containing the monomer unit and an initiator, schematically shown in Fig. 2-1. The homogeneous nucleation theory claims nucleation begins from monomer and initiator solubilized in the dispersion media. A last theory combines homogenous nucleation with coagulation to suggest initial homogenous particle formation, and then further coagulation of the polymer particles.
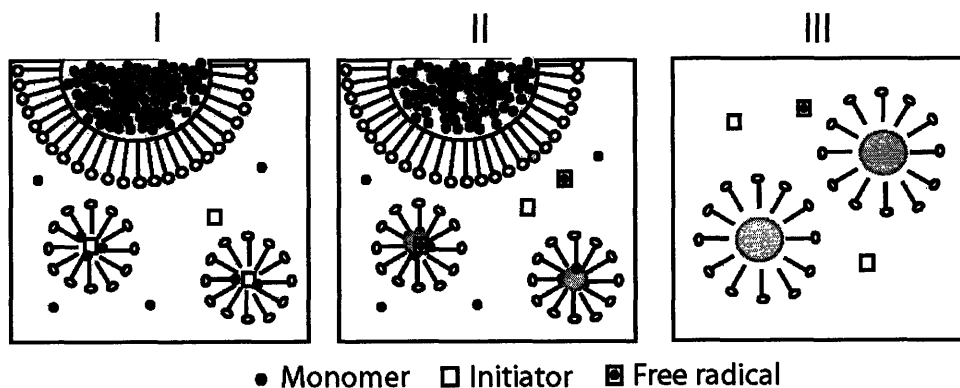

• Monomer   □ Initiator   ▣ Free radical

Figure 2-1: Schematic of micellar nucleation and subsequent polymerization[6].

16

In this work, core-shell (PBA/PS) nanoparticles and core-shell-shell nanoparticles (SiO$_2$/PBA/PS) were synthesized using an emulsion polymerization procedure[15]. Synthesis of the core-shell polymers begins with dispersion of 1.5 g (15% monomer weight) of the cationic surfactant trimethyl(tetra-decyl) ammonium bromide (TTAB, 99%, Aldrich) and 2.5 ml acetone (99.5%, Mallinckdrot) in 75 ml de-ionized water. After stirring and dissolving of the surfactant, 10 g (11.1 ml) butyl acrylate monomer (BA, 99%, Acros) is slowly added to the reactor. Following addition of the monomer, the reactor is closed and placed in an oil bath at 65°C. The emulsion is then vigorously stirred and nitrogen bubbled for at least one hour. Polymerization of the butyl acrylate monomer begins with the addition of 0.1 g of the water-soluble initiator 2,2' azobis (2 methyl propion-amide) dihydrochloride (V50, 97%, Aldrich) in 5 ml of de-ionized water. The reaction is allowed to run for 24 hours, after which an aliquot of the core synthesis is taken. A second emulsion of the polystyrene shell monomer is prepared using 75 ml de-ionized water, 2.06 g TTAB, 13.75 g (15.1 ml) of styrene monomer (S, 99%, Alfa Aesar) and 0.05 ml 1-dodecanethiol (98%, Aldrich) chain transfer agent. The styrene emulsion is nitrogen bubbled and vigorously stirred for at least one hour. Using a nitrogen pressure pump to control the addition rate, the styrene emulsion is dripped into the initial emulsion at a rate of 2-3 drops/second. Once all of the styrene emulsion has been added to the reactor, the reaction is allowed to continue for another 24 hours. The reactor is removed from the oil bath, and the finished polymer is precipitated in methanol, and washed in a 50/50 methanol/water mixture. The powder is then dried in a vacuum oven at room temperature for 2-3 days, to remove the methanol and water.

In the case of core-shell-shell nanoparticles, the polymerization was carried out as described above, except that the hydrophobic SiO_2 particles were mixed into the initial emulsion after the surfactant had been sufficiently dissolved.

2.2 Hydrophobization of SiO_2 nanoparticles

Surface treatment of the silica nanoparticles was completed using Gelest Siliclad®, a pre-made mixture of octadecylsilane derivatives, tertiary alcohols and diacetone alcohol that reacts with water to form a silanol prepolymer. Upon curing, the prepolymer reacts with hydroxyl groups on the silica surface to form the hydrophobic coating. A 1% (by vol.) dilution of Siliclad® solution is prepared in de-ionized water, and subsequently filtered through a 0.22 micron filter to remove precipitates and solids. A gram of silica nanoparticles (99.5%, Aldrich) averaging 15 nm in diameter is then added to 100 mL of the 1% Siliclad® dilution. The mixture is stirred for 5 minutes and then centrifuged at 30,000 rpm for 10 minutes to separate the nanoparticles from the solution. The separated solution is then decanted, and the remaining silica nanoparticles are then cured at 100°C for 5 min under 30 in Hg. (1 atm) vacuum.

2.3 Characterization methods

Dynamic light scattering (DLS) was performed on both core-shell and core-shell-shell nanoparticles to determine particle size. The apparatus used was a ZetaPALS particle sizer (BrookHaven Instruments Co.) with a 676 nm laser source.

Small-angle X-ray scattering (SAXS) is useful in determining information about microphase-separated systems. The scattering peak observed in microphase-separated systems is a result of constructive interference of the x-rays due to the periodicity of the

phase separated domains[16]. In SAXS, the intensity of the x-rays is plotted against the

wavevector q (nm^{-1}), which can be related to some dimension d through the relationship:

$$d \approx 2\pi/q \qquad (2.1)$$

This d spacing is a rough approximation of the particle size in core-shell nanoparticle

systems[6]. X-ray scattering was performed at the Institute for Soldier Nanotechnology,

using a Molecular Metrology (Northampton, MA) instrument consisting of a Cu Kα x-ray

source (λ=1.542 Å), 3-pinhole-collimated beam of diameter ~0.6 μm, and a 2D gas-

proportional, multi-wire Gabriel detector at 1.465 m from the sample.

2.4 Processing Methods

Processing of the core-shell baroplastics was done using compression molding

techniques. In compression molding, the polymer pre-form or powder is placed between

two parts of a mold. The upper mold is lowered onto the lower mold, and the polymer is

compressed as seen in Figure 2-2.
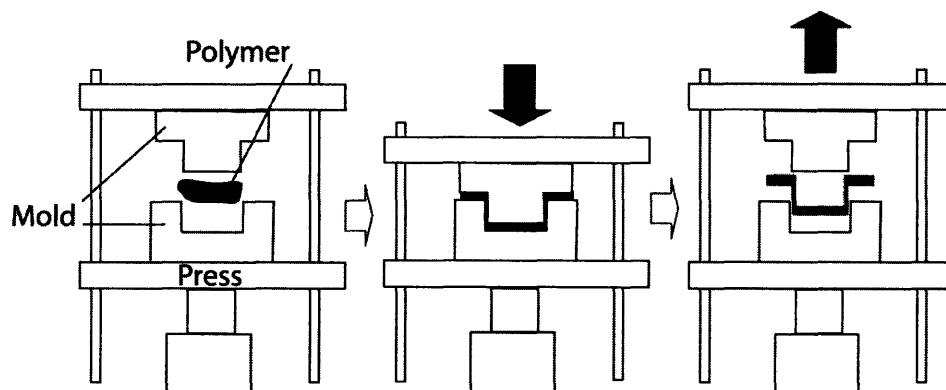
Figure 2-2: Compression molding schematic[6].

A flat aluminum mold, with a 1 mm spacing when closed, was custom made at the MIT Machine Shop. The pre-processed powder was compression molded in the flat mold using a Grimco hydraulic press with a temperature controller. All samples were processed at 25°C, 5000 psi (34.5 MPa), for 5 min.
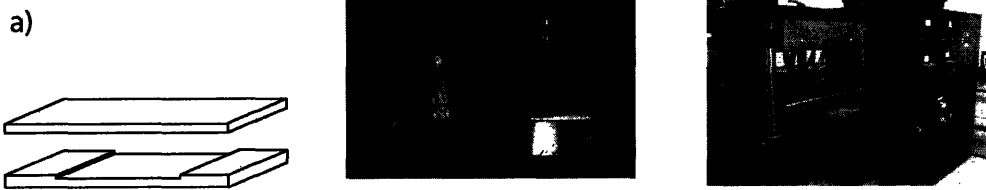

Figure 2-3: a) Schematic of mold parts; b) flat plate aluminum mold; c) hydraulic press[6]

Chapter 3

Pre-Emulsion Incorporation

3.1 Pre-emulsion synthesis strategy

As a first attempt, pre-emulsion incorporation was tried using unmodified silica. This incorporation resulted in very poor synthesis. The core synthesis with unmodified silica led to early precipitation of the PBA core in the reactor, and subsequent termination of the reaction. This is most likely due to the fact that the silica was not entering the surfactant micelles, and being properly incorporated into the core particles. Instead, the negatively charged silica particles interacted with the positively charged surfactant coating on the PBA nanoparticles, causing agglomeration of both the silica and the PBA core particles, until the PBA fell out of solution.

To counteract this, the hydrophobized SiO_2 was incorporated into the core-shell synthesis, with the idea that the silica would enter into the surfactant micelles and be stabilized. Then the reaction would continue on with butyl acrylate monomer entering into the micelles and polymerizing around the SiO_2 nanoparticles. A schematic of this idea is depicted in Figure 3-1.
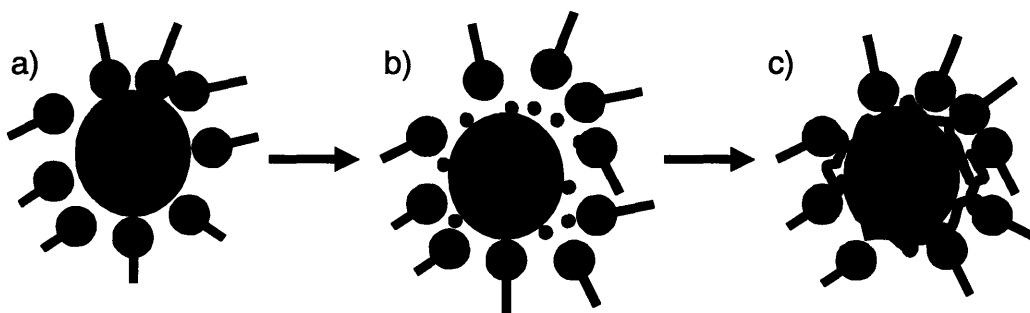

Figure 3.1: Schematic illustrating a) incorporation of SiO_2 into micelle; b) addition of BA molecules into micelle; c) polymerization around SiO_2 nanoparticles.

Incorporation was attempted with two different amounts of hydrophobized silica, 5 wt% and 2 wt%, relative to the polymer components.

3.2 Dynamic Light Scattering

Dynamic light scattering showed a reduction in particle sizes with the incorporation of silica nanoparticles. Table 3.1 shows values from light scattering data taken for PS/PBA, PS/PBA/SiO$_2$ (5%) and PS/PBA/SiO$_2$ (2 %).

Table 3-1: Particle sizes for varying compositions of SiO$_2$

PS/PBA	88 nm
PS/PBA + 5 wt% SiO$_2$	54 nm
PS/PBA + 2 wt% SiO$_2$	53 nm

A typical core-shell emulsion normally yields particles in the 80-100 nm particle size range. With the addition of silica, there is a considerable reduction in particle size. This reduction in particle size is unexpected, considering the addition of 15 nm silica nanoparticles. One possible explanation for this phenomenon is that the amount of silica added is in great excess of the number of surfactant micelles. A rough calculation based on the density of the polymer particles and the mass of the sample shows that there are approximately 2.8 x 10^{15} particles per gram in a typical emulsion. Assuming that all particles nucleate from surfactant micelles, then that value corresponds to the number of micelles present in the solution as well. A calculation for the amount of silica added gave 1.3 x 10^{16} particles per gram of polymer for the 5 wt% addition, and 6x10^{15} particles per gram for the 2 wt% addition. Respectively, the 5 wt% has 4x as many and the 2 wt% has 2x as many surfactant micelles. Once all of the surfactant micelles have one or two silica

nanoparticles, the excess silica nanoparticles start to act as nucleation sites for the formation of polymer particles, without the micelle. For a given amount of initial monomer, excess nucleation sites will cause the amount of polymer per particle to be lower, subsequently making the average particle size smaller.

To test this hypothesis, a third nanocomposite was made with 0.05 wt% silica. At this weight percentage, the number of silica nanoparticles was approximately equal to the number of surfactant micelles. The idea behind this experiment was that by reducing the amount of silica, the particle size should increase. However, this was not the case for the low incorporation experiment, which yielded a similar particle size of 52 nm. This shows that the incorporation of SiO_2 may only be providing excess nucleation sites, and not actually incorporating into the micelles as was expected. Further experimentation would be necessary to understand the mechanism by which this reduction in particle size is occurring.

3.3 Processing of core-shell-shell nanoparticles.

The processing of each silica composition turned out to be very poor. While processing did yield fully formed samples, as with normal core-shell baroplastics, the samples were too brittle and lacked the mechanical integrity of the normal core-shell baroplastics. The samples were so poor that mechanical testing could not even be done on them. Each sample turned out to be very opaque, as exemplified by the 5 wt% incorporation in Figure 3-2. The opaqueness is indicative of macrophase separation of the silica nanoparticles from the rest of the polymer samples. This phase separation gives an explanation as to why the mechanical properties are so poor. The phase separated

silica domains have poor interfacial interactions with the polymer domains and this lack of interaction leads to poor mechanical strength.
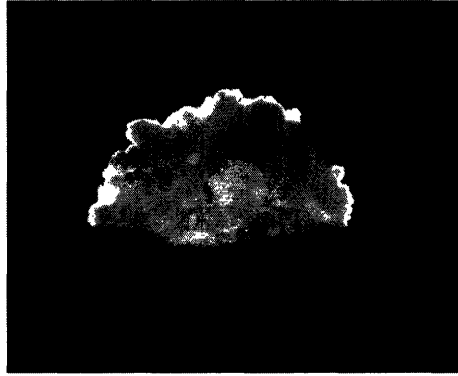

Figure 3-2: Processing of PS/PBA + 5 wt% SiO_2. Processed at 25°C, 5000 psi, 5 min

Chapter 4

Post-Emulsion Incorporation

4.1 Post-emulsion incorporation strategy

The intention of post-emulsion incorporation was to incorporate the silica

nanoparticles in a manner such that they are held in an ordered array amongst the core-

shell particles and subsequently well-dispersed. The proposed strategy was to mix the

silica nanoparticles after the core-shell particles were polymerized, but before

precipitation, such that the silica formed a coordinated 3-D crystalline structure with the

core-shell nanoparticles. This structure, schematically shown in Figure 4-1, would be

based on the untreated silica nanoparticles having a negative surface charge, while the

core-shell nanoparticles have a positive charge as a result of the cationic surfactant that is

used during emulsion polymerization.

The next step in this incorporation strategy was tailoring the radius ratio of the

two nanoparticle types to achieve a particular crystal structure. For 70 nm core-shell

nanoparticles, and 20 nm silica nanoparticles, the radius ratio between the two is 0.285.

This radius ratio corresponds to the silica nanoparticles being tetrahedrally coordinated

by the core-shell nanoparticles[17], as depicted in Figure 4-1.

The final expected crystal structure depends on two more factors. The first is the

molar ratio of the silica and core-shell nanoparticles. For simplicity, a 1:1 molar ratio was

chosen. The final factor depends on what closed-packed structure the core-shell particles

take. Based on the molar ratio and the coordination, the crystal structure will be a

zincblende structure if the core-shell particles take on a face centered cubic (FCC)

packing[17]; if the system takes on a hexagonal closed packed (HCP) structure, then the expected crystal structure will be a wurtzite structure [17].
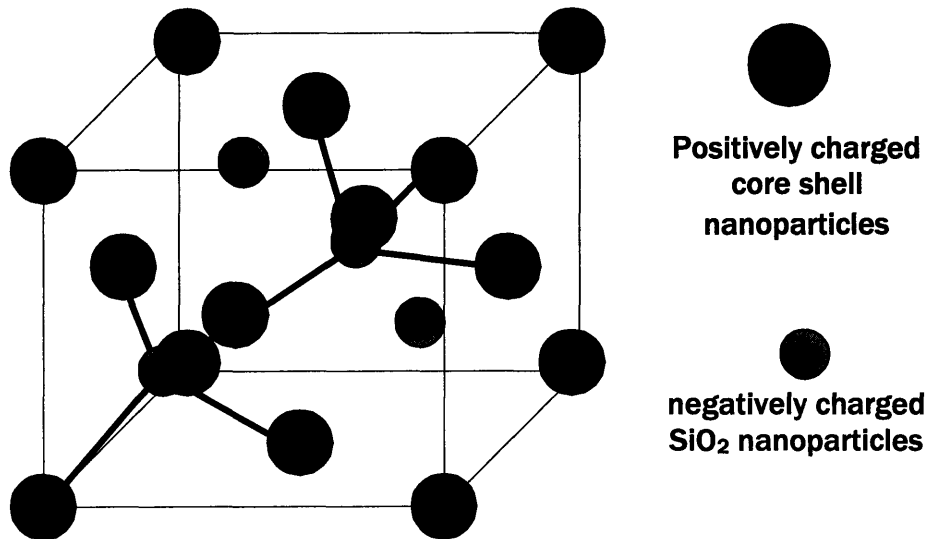

Figure 4-1: Schematic of SiO_2 and core shell nanoparticles in zincblende structure. Figure shows tetrahedral coordination for two of the four SiO_2 nanoparticles.

4.2 Processing of post-emulsion core-shell/SiO₂

Processing of the core-shell/SiO₂ showed a very poorly formed sample. As seen in Figure 4-2, most of the polymer powder only compacted and didn't fully form. The regions of the sample that were able to form under pressure were very opaque and brittle. While this may be a result of silica phase separation, and hence poor interphase interaction, it should be noted that the polystyrene content of this sample was high (75 %), a factor which often leads to poor processing[6]; consequently, the poor processing may not be related to silica phase separation.
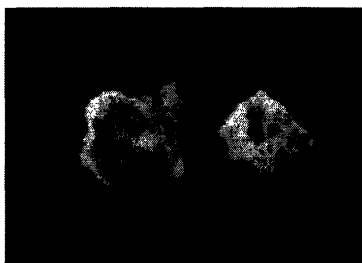
26

Figure 4-2: PS/PBA + SiO$_2$ in a 1:1 molar ratio. Processed at 25°C, 5000 psi, for 5 min

4.3 SAXS on post-emulsion core-shell/SiO$_2$

To determine silica and core-shell structure, SAXS was performed on as dried and processed samples, as shown in Figure 4-3. SAXS data taken on both as dried and after processing samples showed no second order peaks, indicating that there is no long-range crystalline order in the samples. Part of the reason for the lack of crystalline formation may have been a loss of surfactant during the precipitation process, in which methanol and water are used to precipitate and wash the polymer. Without the surfactant providing positive charge, the coordination between the silica and core-shell particles is lost. The loss of peak intensity from powder to processing is often seen in PS/PBA core-shell systems, as there is increased mixing between domains, and less distinction between the PS and PBA domains[6].

As shown in Figure 4-3, the peak maxima occur at a q value of 0.195 nm^{-1}. Using Equation 2-1, the corresponding d value is 32 nm. This d value is smaller than the core-shell nanoparticle size (70 nm), yet bigger than the silica nanoparticle size (20 nm). tetragonal coordination, and therefore must represent a SiO$_2$- SiO$_2$ interparticle spacing. From the proposed structure seen in Figure 4-4, the SiO$_2$- SiO$_2$ interparticle spacing would be 35 nm, in good agreement with the experimental value. However, the structure

only exhibits short range order, given the lack of second-order peaks. Due to the higher

electron density of the SiO_2 component, the SAXS data is more sensitive to the SiO_2

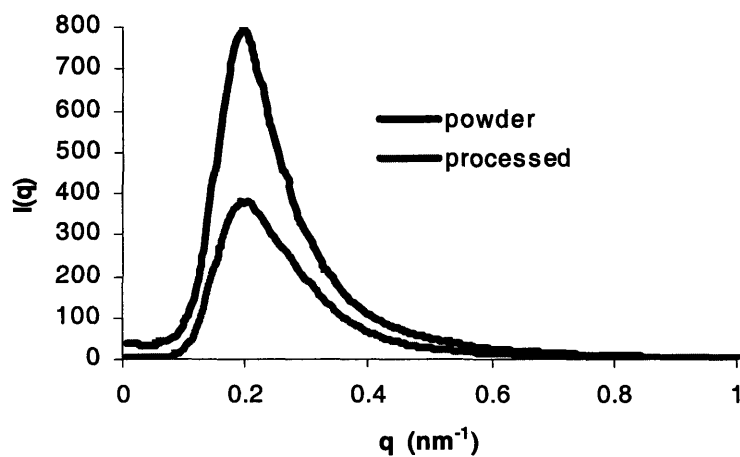interparticle distance than to the PBA core to core distance.

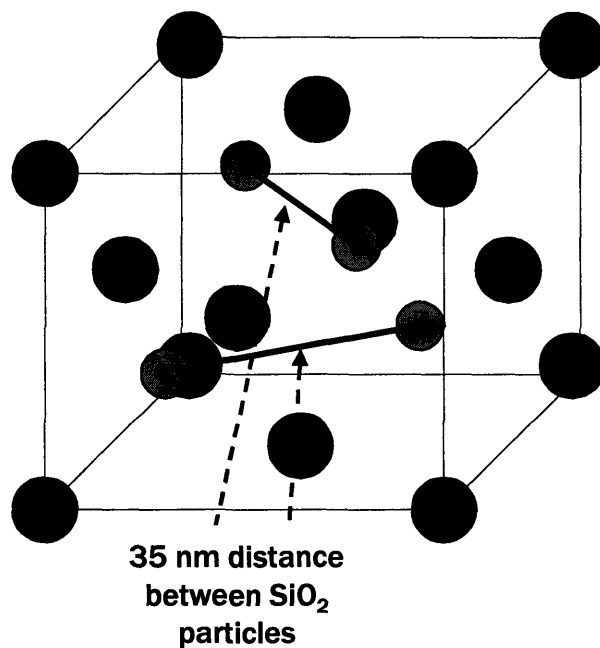**Figure 4-3:** SAXS data for powder and processed samples PS/PBA +SiO_2.

Figure 4-4: Schematic of proposed zincblende structure, with SiO_2-SiO_2 interparticle spacing labeled.

Chapter 5

Conclusions and Future Work

The intention of this work was to show the possibility of incorporating silica nanoparticles into core-shell baroplastics to make them into novel nanocomposite materials that still exhibit low temperature processibility with improved mechanical properties. Two incorporation strategies were devised, one which incorporated silica pre-emulsion synthesis to yield a core-shell-shell morphology, and one that incorporated the silica post emulsion to yield a crystalline coordination between silica and core-shell nanoparticles. While neither strategy yielded the expected results, the role of interfaces and phase separation in baroplastic nanocomposites became more clear, as phase separation tended to create poor interfacial connection, poor inorganic dispersion, and subsequent loss of mechanical strength as compared to typical core-shell baroplastics. From the processed results, we see that dispersion of the silica is essential towards achieving stronger mechanical properties, and clean, transparent, fully formed baroplastic samples.

5.1 Pre-Emulsion Incorporation

Through pre-emulsion incorporation hydrophobized silica nanoparticles are observed to be important towards achieving the goal of a core-shell-shell morphology. Without hydrophobization, the core-shell particles aggregate too early in the process and cause precipitation inside the reactor. Incorporation of the silica has a considerable effect on the particle size, causing smaller particles than typically seen in baroplastic samples. This reduction in particle size could be a result of competing nucleation sites between the surfactant micelles and the silica nanoparticles, though further experiments would be

necessary to determine the exact reason. Other future work using this incorporation scheme could include using other inorganics such as magnetic particles, or quantum dots to achieve new and different properties.

5.2 Post-Emulsion Incorporation

The post-emulsion incorporation results showed that there was no formation of crystalline structure between the silica nanoparticles and the core-shell nanoparticles. This was seen through SAXS, where no second order peaks were found that would indicate longer-range order. However, SAXS data does show a preferred interparticle distance that suggests short range order of silica nanoparticles and core-shell particles, consistent with the proposed zincblende structure. In future work, special care should be made to make sure that the positively charged surfactant isn't washed during the precipitation stage of core-shell synthesis. Once a crystalline structure is achieved, other core-shell/SiO_2 radius ratios, molar ratios, and coordinations could be attempted to determine which crystal structures are best for the mechanical properties of the baroplastic nanocomposite.

References

1. Gonzalez-Leon J. A.; Acar, M. H., Ryu, S.-W. ; Ruzette, A.-V. G. ; Mayes, A. M. "Low temperature processing of 'baroplastics' by pressure-induced flow" *Nature* **2003**, *426*, 424.

2. Jiang, S.; Jiang, W.; Wolf, B.; An, L.; Jiang, B. "Pressure-induced compatibility in PEO/(PEO-*b*-DMS) polymer mixtures". *Macromolecules* **2002**, *35*, 5727.

3. Pollard, M.; Russell, T.P.; Ruzette, A.V.; Mayes, A.M.; Gallot, Y. "The effect of hydrostatic pressure on the lower critical ordering transition in diblock copolymers". *Macromolecules* **1998**, 31, 6493.

4. Ruzette, A.V.G.; Mayes, A.M.; Pollard, M.; Russell, T.P.; Hammouda, B. "Pressure effects on the phase behavior of styrene/n-alkyl methacrylate block copolymers". *Macromolecules* **2003**, *36*, 3351.

5. Ruzette, A.V.G.; Banerjee, P.; Mayes, A.M.; Rusell, T.P. "A simple model for baroplastic behavior in block copolymer melts" *J. Chem. Phys.* **2001**, *114*, 8205.

6. Gonzalez-Leon J.A. "Low temperature processing of baroplastic core-shell nanoparticles and block copolymers." PhD Thesis. **2005**. MIT

7. Gonzalez-Leon J.A. et al. "Core-shell polymer nanoparticles for baroplastic processing." *Macromolecules* **2005** *38* 8036.

8. Castelvetro, V; De Via, C. "Nanostructured hybrid materials from aqueous polymer dispersions." *Adv. in Coll. and Interf. Sci.* **2004**, *108*, 167.

9. Kontou, E.; Niaounakis, M.; "Thermo-mechanical properties of LLDPE/SiO$_2$ nanocomposites." *Polymer.* **2005**. *47* 1267.

10. Bikiaris, D.N.; Papageorgiou, G.Z.; Pavlidou, E.; Nikolaos, V.; Palatzoglou, P.; Karayannidis, G.P. "Preparation by melt mixing and characterization of isotactic polypropylene/SiO$_2$ nanocomposites containing untreated and surface-treated nanoparticles" *J. of App. Poly. Sci.* **2006,** *100,* 2684.

11. Avella, M.; Cafagna, C.; Cerruti, P.; Errico, M.E.; Gentile, G. "Nylon based nanocomposites: influence of calcium carbonate nanoparticles on the thermal stability" *Macromol. Symp.* **2006,** *234,* 163.

12. Zhang, K.; Zheng, L.; Zhang, X.; Chen, X.; Yang, B.; "Silica-PMMA core-shell and hollow nanospheres" *Col. and Surf. A: Physiochem. Eng. Aspects* **2006, 277,** 145.

13. Ramirez, P.L.; Landfester K. "Magnetic polystyrene nanoparticles with a high magnetite content obtained by miniemulsion processes." *Macromol. Chem. Phys.* **2003,** *204,* 22.

14. Shastry, V.; Garcia-Rubio, L. H.; "Identification of nucleation loci in emulsion polymerization processes. I. New information from spectroscopy studies." *J. App. Poly. Sci.* **2006,** *100,* 2847.

15. Ha, J.W.; Park, I. J.; Lee, S.B.; Kim, D. K. "Preparation and characterization of core-shell particles containing perfluoroalkyl acrylate in the shell". *Macromolecules* **2002,** *35,* 6811.

16. Sibayama, M.; Jinnai, H.; Hashimoto, T. in "Experimental methods in polymer science. Modern methods in polymer research and technology" (Tanaka, T. ed.) Academic press, San Diego CA, **2000**. Chap.2. pg. 105-114, 124-139.

17.   Chiang, Y.M. ; Birnie, D.P.; Kingery, W.D. "Physical Ceramics: Principles for ceramic science and engineering" J Wiley, New York, **1997**. Chap.1. pg. 13-17 20-22.